energies

Article

Pore Structure and Fractal Characteristics of Continental Low Maturity Organic-Rich Shale in the Sha-4 Member of the Liaohe Western Depression

Yinglin Liu [1], Lei Zhang [1,*], Xuejuan Zhang [1], Xin He [2], Jinpeng Li [3], Yabing Xing [1], Fuxin Jin [1] and Yiran Wang [1]

[1] School of Petroleum Engineering, Chongqing University of Science & Technology, Chongqing 401331, China
[2] College of Petroleum Engineering, Xi'an Shiyou University, Xi'an 710065, China
[3] Exploration and Development Research Institute of Liaohe Oilfield, Panjin 124010, China
* Correspondence: zhlkeyan@163.com

Abstract: The research on pore structure and heterogeneity of shale reservoirs has always been a hotspot in the study of unconventional reservoir characteristics. China is a country dominated by continental shale. Compared with marine shale, continental shale has lower maturity and stronger reservoir heterogeneity. In this study, Sha-4 shale in the Liaohe Western Depression was selected for low-temperature nitrogen adsorption, scanning electron microscopy and other experiments revealing the pore structure and fractal characteristics of continental low mature organic-rich shale. The fractal dimension was calculated by the FHH model and the effects of TOC and mineral composition on pore structure and fractal characteristics were discussed. The results show that the Sha-4 shale in the study area is mainly mesoporous and the main pore types are inorganic pores with relatively large pore diameters, such as intergranular pores and inter-crystalline pores. The pore morphology is very complex, mainly narrow slit and flat pore, and the pore is often filled with organic matter. The fractal dimensions D_1 range from 2.58 to 2.87 and D_2 range from 2.18 to 2.55, and the pore structure shows obvious dual fractal characteristics. The pore structure and fractal characteristics of shale are mainly affected by TOC and quartz due to the low degree of the thermal evolution of shale and their effects are different from those of marine shale reservoirs. The increase in TOC reduces the heterogeneity of the shale reservoir. In addition, mineral particles with strong weathering resistance and stability such as quartz can protect the pore structure of shale, improve the pore structure and reduce the reservoir heterogeneity. This study can provide support for the study of low maturity continental shale reservoir heterogeneity in the Sha-4 member of the Liaohe Western Depression.

Keywords: continental low mature organic-rich shale; pore structure; fractal feature; Liaohe Western Depression; Sha-4 shale; unconventional shale reservoirs

Citation: Liu, Y.; Zhang, L.; Zhang, X.; He, X.; Li, J.; Xing, Y.; Jin, F.; Wang, Y. Pore Structure and Fractal Characteristics of Continental Low Maturity Organic-Rich Shale in the Sha-4 Member of the Liaohe Western Depression. *Energies* **2023**, *16*, 327. https://doi.org/10.3390/en16010327

Academic Editors: Xixin Wang, Xiaoyue Cao, Xun Zhong and Reza Rezaee

Received: 23 November 2022
Revised: 18 December 2022
Accepted: 24 December 2022
Published: 28 December 2022

1. Introduction

Shale oil has the characteristics of source-reservoir integration [1–5], as both a source rock and a reservoir, and the micro-pore structure of shale-rich reservoir rocks have an important impact on shale oil reservoir physical properties and oil content [2,3]. A correct understanding of reservoir micropore structure can guide shale oil exploration and development. At the micro-scale, the distribution and relative quantity of shale mineral components, the type, distribution, pore diameter and morphology of pores and micro-cracks have significant heterogeneity [4]. The characterization of pore structure and the heterogeneity of shale reservoirs have always been hot issues in shale oil reservoir research. In terms of reservoir pore structure characterization, scanning electron microscopy, nitrogen adsorption, high-pressure mercury injection and nuclear magnetic resonance are commonly used to characterize pore morphology, pore size, pore throat distribution, etc. [5]. In terms of research on the heterogeneity of pore structure, the main goal is to obtain pore structure parameters based on the reservoir characterization technology, calculate fractal dimension by combining fractal theory [6–8] and conduct quantitative analysis on the roughness of pore surface and uniformity of pore development [9–11].

Predecessors have carried out much research work on the pore structure and fractal characteristics of shale in different areas and have made significant achievements. Xiong Jian et al. studied the pore structure and fractal characteristics of Longmaxi Formation shale samples in Changning, Sichuan Basin based on nitrogen adsorption experiments and fractal theory [7]; Nie Wancai et al. studied the influence of mineral components of marine terrestrial transitional coal shale, in the Taiyuan Formation in Qinshui Basin, on pore structure and fractal characteristics [11]. However, previous studies mainly focused on marine shales such as Longmaxi Formation and Longtan Formation and marine terrestrial transitional shale such as Taiyuan Formation, while the research on pore structure and fractal characteristics of continental shale are less common, and especially that on low maturity continental shale is very weak.

Liaohe Western Sag is rich in shale oil and gas resources, with good exploration and development potential [12,13]. In recent years, a large number of scholars have carried out much basic research on shale oil reservoir characteristics and reservoir forming conditions for the Sha-4 member in the Liaohe Western Depression. Ge Mingna et al., based on research into the influencing factors of shale oil and gas, revealed the main controlling factors of shale oil and gas enrichment in the Shahejie Formation by using the method of multifactor comprehensive evaluation and partial factor focus analysis [14]. Yang Chao et al. used scanning electron microscope-focused ion beam (FIB-SEM), helium gas adsorption-desorption, X-ray diffraction analysis, kerogen microscopy and other organic geochemical experiments to discuss shale reservoirs, from microscopic pore structure to the significance of reservoir formation [15]. Based on laboratory tests of a large number of shale samples, Shan Yansheng et al. analyzed the conditions for shale oil and gas enrichment in the Liaohe Western Depression of the Bohai Bay Basin and discussed the characteristics and patterns of shale oil and gas distribution in continental rift basins [16]. Other scholars have studied the origin and distribution of thin sand layers in shale oil reservoirs in the Liaohe Western Depression [17,18].

However, there is little research on reservoir characteristics on the micro scale. In this paper, shale in the western slope area of Liaohe western sag is taken as the research object, to fill the gap regarding current reservoir micropore structure characteristics; based on nitrogen adsorption experiments, the reservoir pore structure is characterized and the shale pore fractal dimension is calculated. The effects of organic carbon content and mineral composition on shale pore structure and fractal characteristics are discussed, respectively. This study will enrich and improve the research theory into continental shale and provide a certain reference value for research into the influence mechanism of micropore structure fractal characteristics of continental low mature shale reservoirs.

2. Geological Setting

Liaohe Western Depression is located in the northeast of Bohai Bay Basin, which is the largest oil-generating sag in the Liaohe Depression of Bohai Bay Basin, an area of about 2530 Km^2 bounded by the western uplift in the west and the central uplift in the east. Tectonically, it can be divided into nine tectonic units (Figure 1a) [17]. The Paleogene Shahejie Formation can be divided into Sha-1, Sha-2, Sha-3 and Sha-4 from top to bottom, from which Sha-4 can be divided into Dujiatai and Gaosheng oil-bearing formations from top to bottom. The basin is strongly rifted and block-faulted and the rate of depressional subsidence is high. During the deposition of the Sha-4 member, the rapid subsidence has resulted in a non-compensated semi-deep-lake-deep-lake depositional environment in all three basins [19], which has developed a huge thickness of dark organic-rich mudstone (Figure 1b). The dark mudstone of the Sha-4 member has a large cumulative thickness and good continuity at moderate burial depths, with an overall distribution: thick in the north and thin in the south, thick in the east and thin in the west [16]. The center of mud shale thickness is mainly located in the northern area The distribution of the mud shale is controlled by the tectonic and sedimentary phases and is mainly developed in the semi-deep lake and deep lake subphase areas in the center of each sub-depression [20].

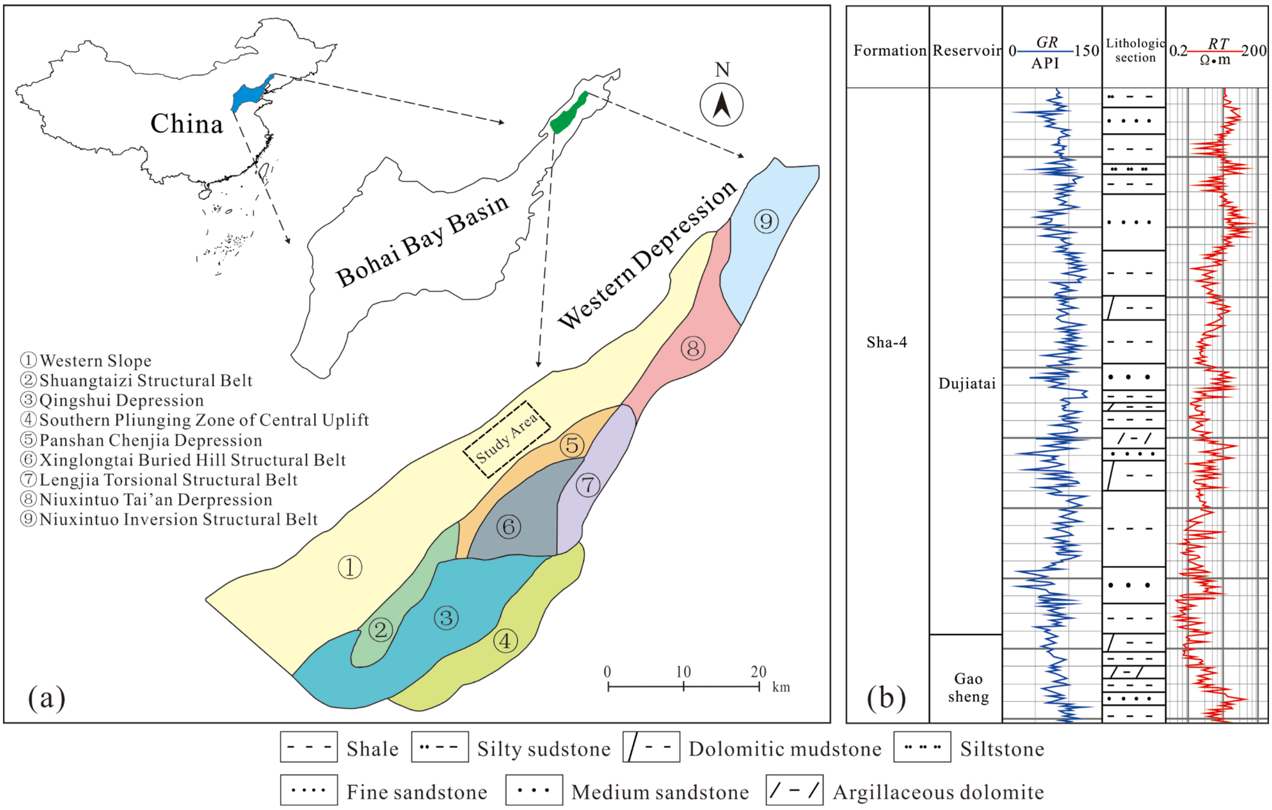

Figure 1. (**a**) Location of the study area; (**b**) Comprehensive histogram of Sha-4 member.

The study area is located in the western slope of the Liaohe Western Depression. During the sedimentation period of the Shahejie Formation, the area experienced several stable sedimentation periods. The sedimentary center is dominated by shallow lake to semi-deep lake surfaces [12]. The interbedding of mudstone or shale and silty fine sandstone or dolomitic carbonate rocks are developed in a large area [18], which is not only an effective source rock of oil and gas-rich sags but also a favorable area for large-scale shale oil accumulation.

3. Samples and Experimental Methods

3.1. Sample Collection

The samples are all taken from the shale reservoir of Sha-4 member in the western slope of Liaohe Western Depression. Due to the complex lithological changes during the sedimentation period in this area, after adequate core observation, a reasonable sampling scheme is designed to ensure the representativeness of the experimental samples and 13 samples are taken in total.

3.2. Experimental Instruments and Lab Analysis

3.2.1. Total Organic Carbon Analysis

The total organic carbon (TOC) of rocks is analyzed by using the CS-230 carbon sulfur analyzer of the American Lik Company (Opelika, AL, USA). Before the experiment, the samples are subject to ultrasonic decontamination, grinding, pickling, low-temperature drying and other treatments. The experimental standard refers to GB/T 19145-2003 Determination of TOC in Sedimentary Rocks.

3.2.2. X-ray Diffraction Analysis

The whole rock quantitative X-ray diffraction analysis adopts a D8-DISCOVER X-ray diffractometer (Figure 2a). The experimental standard refers to the SY/T 5163-2018 analytical method for clay minerals and common nonclay minerals in sedimentary rocks by X-ray diffraction. Before the experiment, the samples were treated with oil washing, low-temperature drying, grinding, etc. The test temperature was 27 °C and the ambient humidity was 40%.

(**a**) (**b**)

Figure 2. The experiment site. (**a**) X-ray diffraction; (**b**) SEM.

3.2.3. Vitrinite Reflectance (Ro%) Measurement

The vitrinite reflectance is measured by the MSP200 vitrinite reflectance meter, Leica, Germany. The instrument has a measuring wavelength of 546 nm, 125× magnification, a reflectance range of 0.1–10.0% and a resolution of 0.1%. Refer to SY/T 5124-2012 Determination of Vitrinite Reflectance in Sedimentary Rocks for the test standard. The test temperature is 25 °C and the ambient humidity is 42%.

3.2.4. Nitrogen Adsorption Experiment

The nitrogen adsorption experiment adopts the ASAP2460 adsorption instrument of the Mack Company in the United States. The aperture measurement range of the instrument is 0.35–500 nm, the minimum specific surface area can be measured to 0.0001 m^2/g and the minimum pore volume can be measured to 0.0001 cm^3/g. Before the experiment, the sample was placed in deionized water for ultrasonic cleaning, the surface impurities were fully removed for low-temperature drying pretreatment, then ground to 20–50 meshes. The powder sample was vacuumized at 120 °C for 12 h. Liquid nitrogen with a purity of greater than 99.99% was used as the adsorption medium and the experiment was carried out at −195.85 °C liquid nitrogen temperature.

3.2.5. SEM Experiment

In the scanning electron microscope (SEM) experiment, Semefer Apero S Hivac scanning electron microscope and Bruker Xflash Detector 6/60 energy spectrometer were used (Figure 2b). After sample pretreatment, argon ion polishing is and then carbon spraying is carried out. The sample is put into SEM for observation and micromineral identification is carried out with an energy spectrometer. In this study, shale samples from the fourth member of the Shahejie Formation were polished by argon ion and their pore development types were observed by SEM.

3.3. Calculation Model of Fractal Dimension

The fractal theory was founded in the mid-1970s to study the fractal characteristics of the internal structure of objects based on their self-similarity [21]. Recently, advanced models were used to calculate the fractal dimension of micropores, mainly including NK (Newton Kantorovich), FHH (Frenkel Halsey Hill) and Neimark and Langmuir models [22–25].

In this study, the FHH model is used to calculate the pore fractal dimension, which is the theoretical calculation model of the fractal dimension proposed by Pfeiferper and others in 1983 based on nitrogen adsorption experimental data. Because of its wide application scope, simple calculation steps and other characteristics, it is the most widely used at present. The formula is as follows:

$$\ln V = K \ln [\ln (P_0/P)] + C \quad (1)$$

where V is the volume of gas adsorbed when the pressure is P, m^3; P—balance pressure; P_0—saturated vapor pressure, MPa; K—slope; C—constant.

According to the measured experimental data of nitrogen adsorption, the above formula is worked out, the slope K is obtained by plotting $\ln V$ versus $\ln [\ln (P_0/P)]$ and the fractal dimension D is equal to K plus 3. The fractal dimension is usually between 2 and 3. The closer the fractal dimension is to 2, the more regular the pore surface and the simpler the pore structure; The closer the fractal dimension is to 3, the more irregular the sample pore surface and the more complex the pore structure [8].

4. Results

4.1. Basic Characteristics of Shale

The basic characteristics of shales in the fourth member of the Shahejie Formation in the study area were analyzed through the analysis of the total organic carbon of rocks, measurement of vitrinite reflectance and thin section identification experiment (Table 1). The shale development types of the Sha-4 member in the study area include mainly massive mudstone, shale, silty mudstone and dolomitic mudstone. Dolomitic mudstone and muddy dolomite are commonly interbedded. The shale is rich in organic matter, with total organic carbon (TOC) of 0.46–4.72%, with an average of 3.069%. According to previous studies, the vitrinite reflectance (Ro) of shales in the Sha-4 member of Liaohe Western Depression is generally 0.2–1.8%, with an average of 0.46% [14]. Ro values of five shale samples are 0.37–0.46%, which shows that shales in the Sha-4 member of the study area are characterized by high TOC and low maturity.

Table 1. Basic information of Sha-4 shale samples.

Samples	TOC (%)	Ro (%)	Lithology
L1	2.46	0.45	Mudstone
L2	0.46	0.38	Silty mudstone
L3	0.47	0.38	Mudstone
L4	2.72	0.37	Mudstone
L5	3.41		Shale
L6	3.88		Silty mudstone
L7	3.48		Shale
L8	4.14		Dolomitic mudstone
L9	4.72		Shale
L10	4.33	0.46	Silty mudstone
L11	3.34		Dolomitic mudstone
L12	3.22		Dolomitic mudstone
L13	3.27		Dolomitic mudstone

The whole rock quantitative X-ray diffraction analysis experiment shows that the shale mineral components of the Sha-4 shale samples are mainly clay minerals and quartz, followed by feldspar and carbonate rock minerals, with less pyrite content (Figure 3).

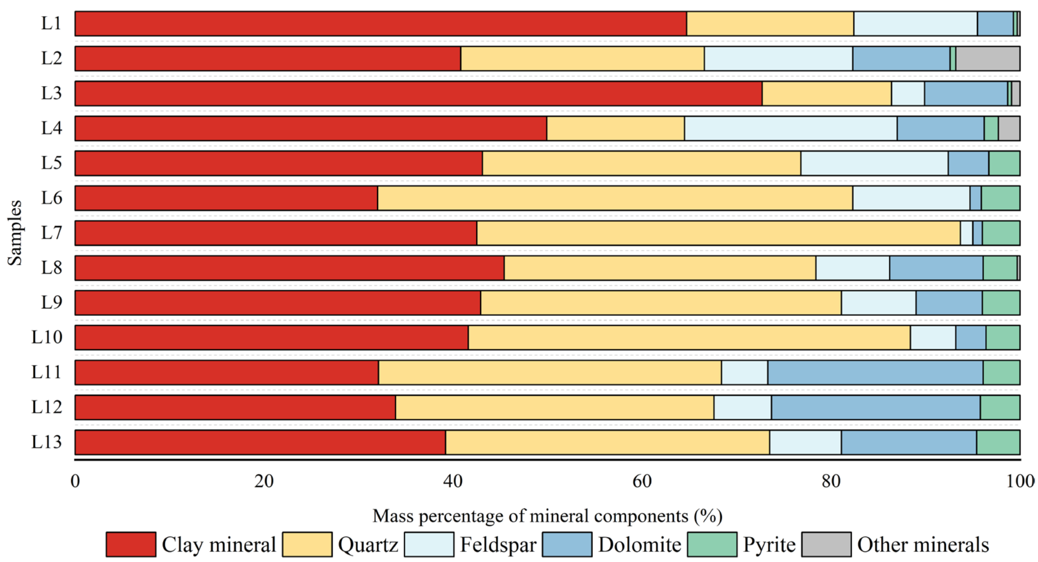

Figure 3. The proportions of mineral composition.

4.2. The Pore Structure Based on SEM

The experimental results show that the Sha-4 shale mainly develops inorganic pores such as intergranular pores, inter-crystalline pores and dissolution pores, while the organic pores are less developed. The pores between mineral particles are often filled with a large amount of organic matter and the pore morphology is narrow and long (Figure 4a).

1. Intergranular pore

The intergranular pores are formed by incomplete cementation between different mineral particles or particle breakage under diagenetic compaction (Figure 4b,c) [15]. It is the most widely developed pore type in the shale reservoir of the fourth member of the Shahejie Formation in the study area, mainly in the form of silt and flat.

2. Inter-crystalline pore

The shaly shale reservoir of Sha-4 shale in the study area is mainly formed by the mutual support of pyrite, dolomite, clay minerals and other crystals and the pores are common with argillaceous fillings and organic matter (Figure 4d–f) [26,27]. The intergranular pores of pyrite are mostly irregular polygon and wedge-shaped and the pore diameter can reach hundreds of nanometers; The inter-crystalline pores of dolomite and clay minerals are mainly slit-shaped and irregular polygons.

3. Dissolution pore

The dissolution pores are mainly the pores formed by the dissolution of unstable minerals such as feldspar and carbonate rocks. Such pores are relatively less developed in the shale of the study area's fourth member of the Shahejie Formation. Most of them are intra-granular dissolution pores formed by the dissolution of unstable minerals. The pore morphology is oval (Figure 4g).

4. Microfracture

The shale fractures of Sha-4 shale in the study area are mainly structural fractures and bedding fractures filled with organic matter (Figure 4h,i). The crack surface of micro cracks is relatively straight and the crack width can reach a micron level.

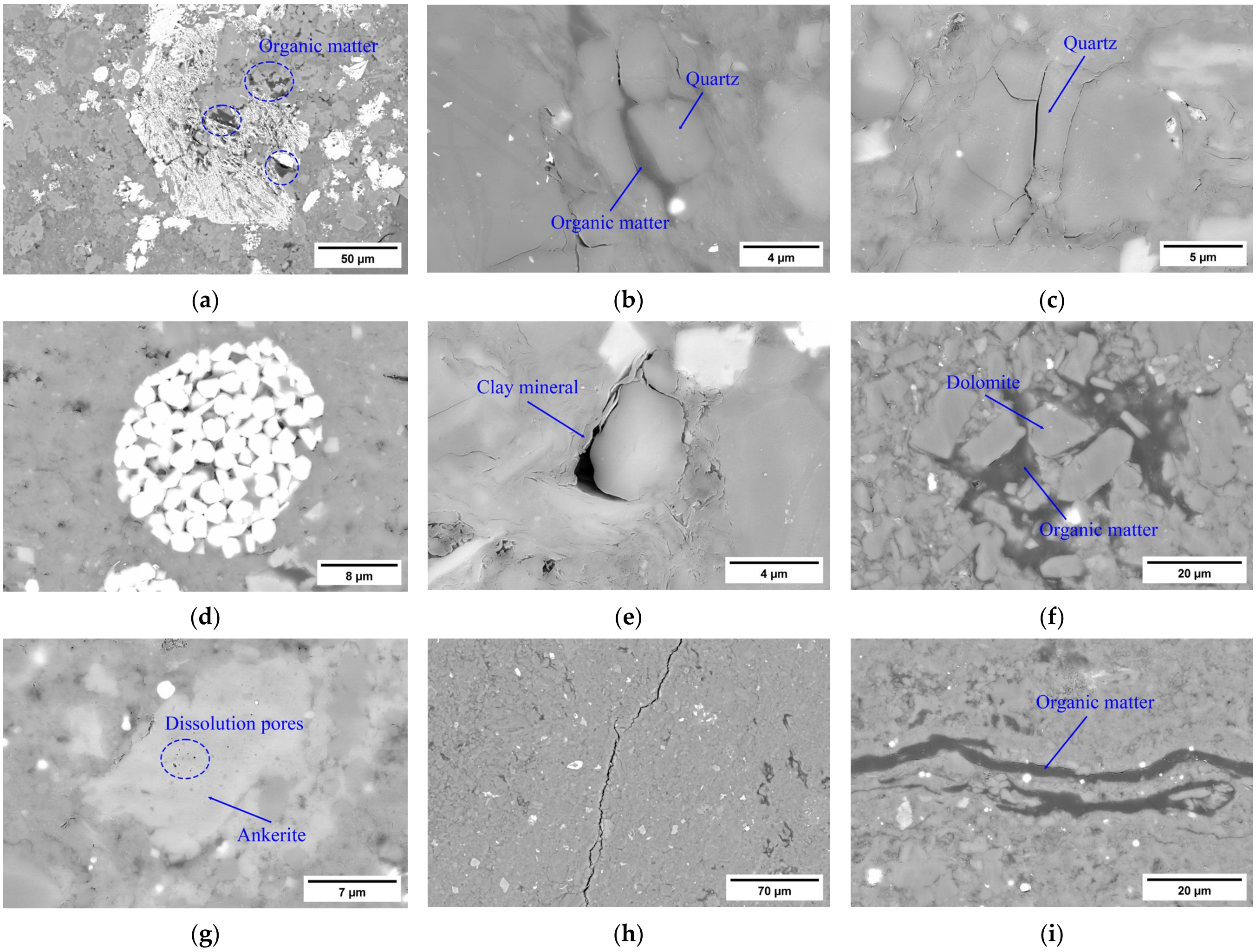

Figure 4. Pore types of Sha-4 shale samples. (**a**) The mineral grains are filled with a large amount of organic matter; (**b**) Intergranular pore filled with organic matter; (**c**) Intergranular pore of quartz; (**d**) Inter-crystalline pores of Pyrite; (**e**) Inter-crystalline pores of clay minerals; (**f**) Inter-crystalline pores of dolomite; (**g**) Dissolution pores of ankerite; (**h**) Microstructural fracture; (**i**) Bedding joint, filled with organic matter.

4.3. The Pore Structure Based on Nitrogen Adsorption

The isotherm adsorption-desorption curves of shale samples show the following characteristics (Figure 5a): The isotherm adsorption curves of 13 shale samples all show an inverse "S" shape, similar to the IV (a) type of IUPAC adsorption isotherm and related to the relatively developed mesopores [28]. With the increase of relative pressure P/P_0, the adsorption capacity increased gradually and the adsorption-desorption curves were nearly parallel. When $P/P_0 > 0.46$, the adsorption-desorption curves are separated into hysteresis loops. Some samples (L2, L3) have a large adsorption capacity when P/P_0 is low.

The Sha-4 shale is dominated by nano-sized pores and the pore size distribution curve is dispersive (Figure 5b), i.e., there are multiple peaks, the pore size is mainly concentrated in the range of less than 50 nm and the peak pore size is mainly 2–5 nm. Among them, L2 and L3 samples have peaks at the range of less than 2 nm, indicating that the micropores of L2 and L3 samples are relatively developed, which verifies the analysis of the characteristics of the adsorption–desorption curve above.

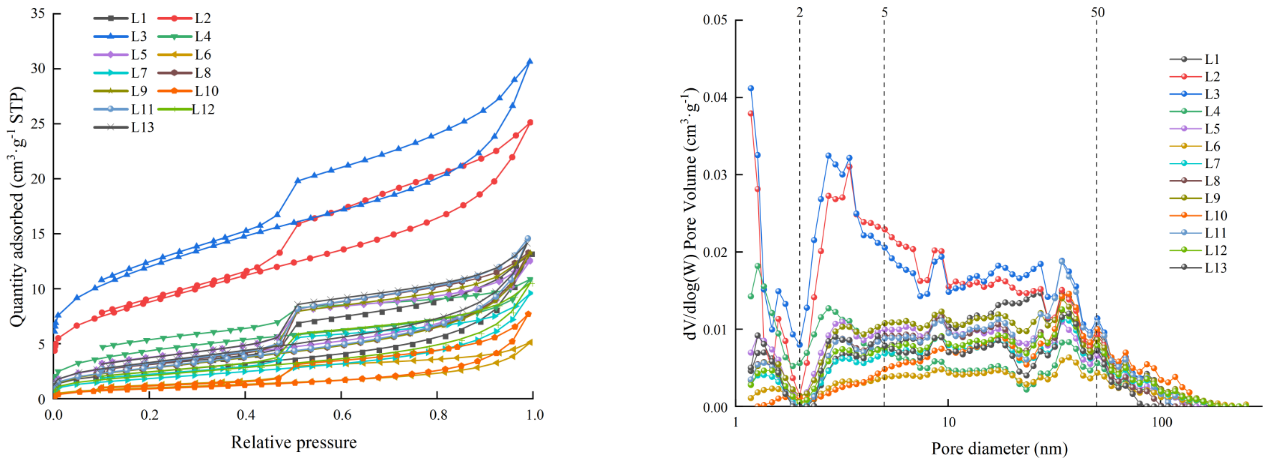

(**a**) (**b**)

Figure 5. (**a**) The nitrogen adsorption–desorption curves of samples; (**b**) Pore size distribution of samples.

According to the calculation results (Table 2), the pore specific surface area of Sha-4 shale is 3.6219–42.2139 m^2/g, average 13.4228 m^2/g; The average pore diameter is 5.2087–12.7806 nm, average 7.6392 nm; total pore volume is 0.0078–0.0404 cm^3/g, average 0.0197 cm^3/g.

Table 2. Pore structure parameters of samples.

Samples	Specific Surface Area ($m^2 \cdot g^{-1}$)	Average Pore Diameter (nm)	Total Pore Volume ($cm^3 \cdot g^{-1}$)
L1	8.8289	7.5153	0.0153
L2	31.3820	5.7121	0.0351
L3	42.2139	5.5876	0.0404
L4	15.6083	5.2087	0.0146
L5	11.7083	7.0119	0.0187
L6	3.6219	8.8733	0.0078
L7	6.7976	8.7588	0.0147
L8	10.2120	7.9057	0.0204
L9	10.2930	7.8625	0.0204
L10	3.3829	12.7806	0.0120
L11	10.4524	8.5238	0.0224
L12	7.8650	6.2164	0.0122
L13	12.1300	7.3528	0.0215

4.4. Fractal Dimension

According to the adsorption–desorption curve, a hysteresis loop occurs when $P/P_0 > 0.46$. It can be seen that the two specific pressure zones, $P/P_0 < 0.46$ and $P/P_0 > 0.46$, reflect two different gas adsorption mechanisms [29]. The different gas adsorption mechanisms also indicate that the pore structure indicated before and after the relative pressure is significantly different, that is, there is a dual fractal feature. The appearance of dual fractal characteristics indicates that the sample pore fractal dimension has a pore size boundary used to divide two pore types and their pore structures have obvious differences [7]. In this study, $P/P_0 = 0.46$ is used as the boundary line to divide the high specific pressure zone ($0.46 < P/P_0 < 1$) and the low specific pressure zone ($0 < P/P_0 < 0.46$). Two different specific pressure zones represent the pores with larger pore diameters and the pores with smaller pore diameters, which are called macropores and small pores, respectively.

The plot of $\ln V$ versus $\ln [\ln (P_0/P)]$ is obtained based on the FHH model (Figure 6). Scatter data are distributed on the two curves and the piecewise linear fitting correlation is good. The correlation coefficient R^2 is above 0.92, indicating that the shale pores in the fourth member of the Shahejie Formation have obvious dual fractal characteristics. The fractal dimension D_1 of macropores and the fractal dimension D_2 of micropores are calculated, respectively (Table 3). D_1 is 2.58–2.87, with an average of 2.75; D_2 is 2.18–2.55, with an average of 2.38; the pore structure of macropores is more complex.

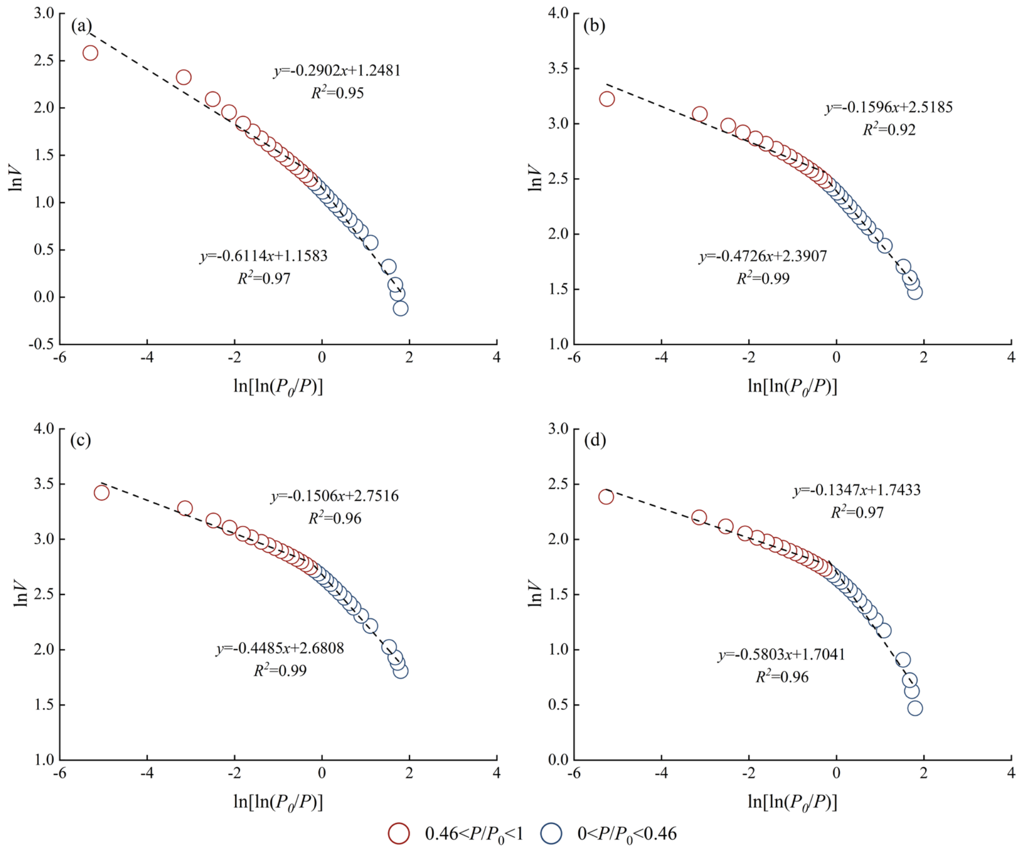

Figure 6. Sectional fitting diagram of ln$V$ and ln [ln (P_0/P)] of typical samples. (**a**) Sample L1; (**b**) Sample L2; (**c**) Sample L3; (**d**) Sample L4.

Table 3. Shale pore fractal dimension based on the FHH model.

Samples	High Specific Pressure (0.46 < $P/P0$ < 1)			Low Specific Pressure (0 < $P/P0$ < 0.46)		
	K	R^2	D_1	K	R^2	D_2
L1	−0.29	0.95	2.71	−0.61	0.97	2.39
L2	−0.16	0.92	2.84	−0.47	0.99	2.53
L3	−0.15	0.96	2.85	−0.45	0.99	2.55
L4	−0.13	0.97	2.8	−0.58	0.96	2.42
L5	−0.22	0.94	2.78	−0.60	0.98	2.40
L6	−0.27	0.95	2.73	−0.67	0.97	2.33
L7	−0.27	0.95	2.73	−0.63	0.98	2.37
L8	−0.29	0.97	2.71	−0.63	0.99	2.37
L9	−0.25	0.94	2.75	−0.66	0.98	2.34
L10	−0.42	0.98	2.58	−0.82	0.97	2.18
L11	−0.31	0.98	2.69	−0.63	0.99	2.37
L12	−0.26	0.95	2.74	−0.65	0.98	2.35
L13	−0.27	0.98	2.73	−0.61	0.99	2.39

5. Discussion

5.1. Pore Types and Pore Size Distribution Characteristics

The IUPAC (International Union of Pure and Applied Chemistry) reclassified the standard hysteresis loop types in 2015 (Figure 7) [28]: H1 hysteresis loop absorption and desorption curves are very steep and nearly perpendicular to the coordinate axis, reflecting cylindrical pores with narrow and uniform pore size distribution; the H2 hysteresis loop reflects the relatively complex pore structure. The H2 (a) desorption curve is very steep, which is caused by the blockage of the narrow pore neck. The H2 (b) is also caused by the blockage of the pore neck, but the width of the pore neck is large. The former is mainly a thin-necked ink bottle pore and the latter is a wide-necked ink bottle pore. The curves of H3 type hysteresis loop adsorption and desorption are parallel to each other and the adsorption and desorption amount are almost linearly related to P/P_0, rising slowly with the increase in P/P_0, reflecting the flat pores formed by the stacking of plate-like particles. The H4 hysteresis loop is similar to the H3 hysteresis loop, but there is a large adsorption capacity when P/P_0 is low, which is related to the development of micropores, and the pore shape is slit. The H5 hysteresis loop is rare, which reflects that there are both closed pores and open pores in the sample and the pore structure is very complex. IUPAC divides pores into three categories according to pore size [28]: micropores with a pore size less than 2 nm, mesopores with a pore size between 2 and 50 nm and macropores with a pore size greater than 50 nm.

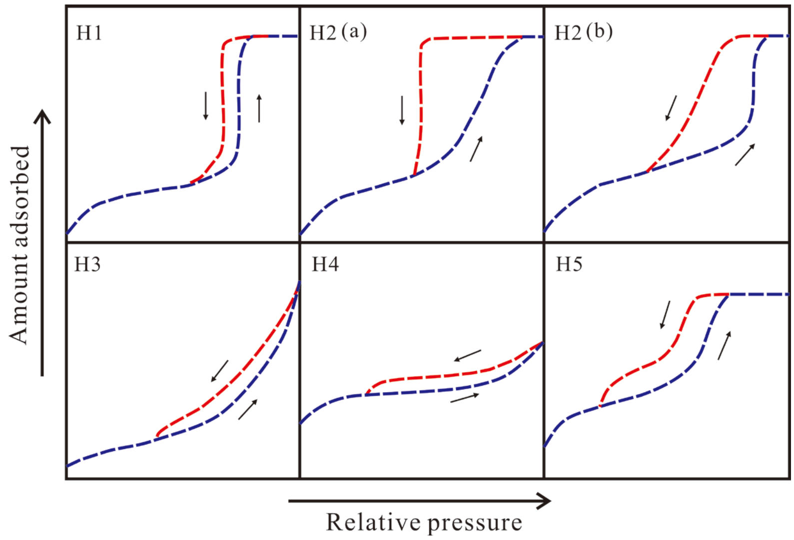

Figure 7. IUPAC hysteresis loop morphological classification [28].

The pore structure of shale is very complex and the pore morphology is different, so the hysteresis loop formed cannot completely conform to a certain type, but is a complex of two or more types [30]. Therefore, the Sha-4 shale has a high degree of pore opening and the hysteresis loop shape has the characteristics of H3 and H4 types. The pore shape is mainly flat and slit. The pore size of the Sha-4 shale is mainly concentrated in the range of less than 50 nm and is mainly mesoporous, with few micropores and macropores.

5.2. Factors Influencing Pore Structure

The correlation analysis of pore structure parameters, TOC and mineral components of shale samples from the fourth member of the Shahejie Formation in the study area was conducted. The pore specific surface area of shale is significantly negatively correlated with TOC (Figure 8a), with a correlation coefficient R^2 of 0.78. The correlation with clay mineral quartz content is weak (Figure 8b,c), with R^2 of 0.35 and 0.45, respectively. This shows that the specific surface area of pores is mainly affected by the TOC; the higher the TOC is, the smaller the specific surface area is. Mineral components have a certain influence on the specific surface area of pores. The less clay mineral, the more quartz and the smaller the specific surface area of pores. The average pore diameter shows a weak positive correlation with TOC and quartz (Figure 9a,c), R^2 is 0.40 and 0.54, respectively, and does not correlate with clay mineral (Figure 9b). This shows that the higher the TOC and the more quartz, the larger the average pore diameter. The total pore volume shows a significant negative correlation with TOC (Figure 10a), R^2 is 0.58 and the correlation with clay minerals and quartz is weak (Figure 10b,c); R^2 is 0.23 and 0.30, respectively. This shows that the total pore volume of shale is mainly affected by TOC and the total pore volume decreases with the increase in TOC.

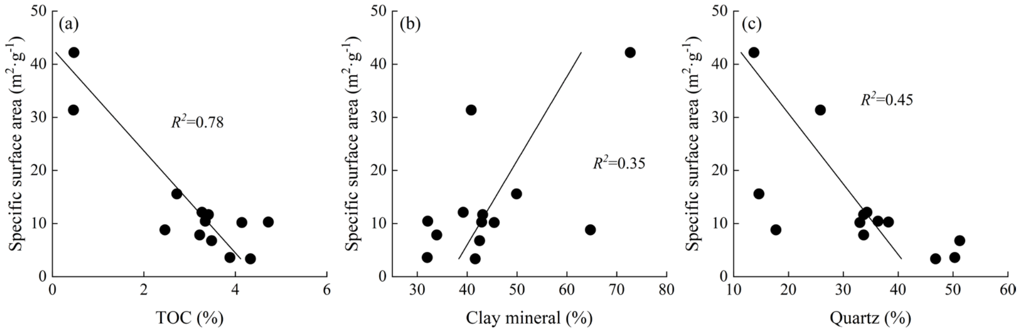

Figure 8. (**a**) Relationship between specific surface area and TOC; (**b**) Relationship between specific surface area and clay mineral; (**c**) Relationship between specific surface area and quartz.

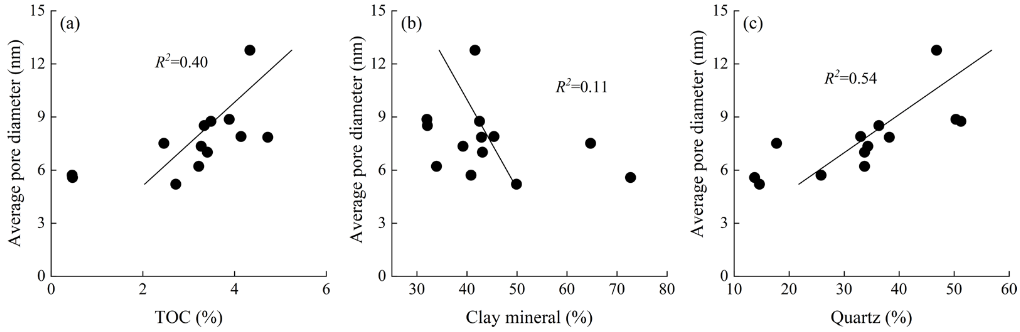

Figure 9. (**a**) Relationship between average pore diameter and TOC; (**b**) Relationship between average pore diameter and clay mineral; (**c**) Relationship between average pore diameter and quartz.

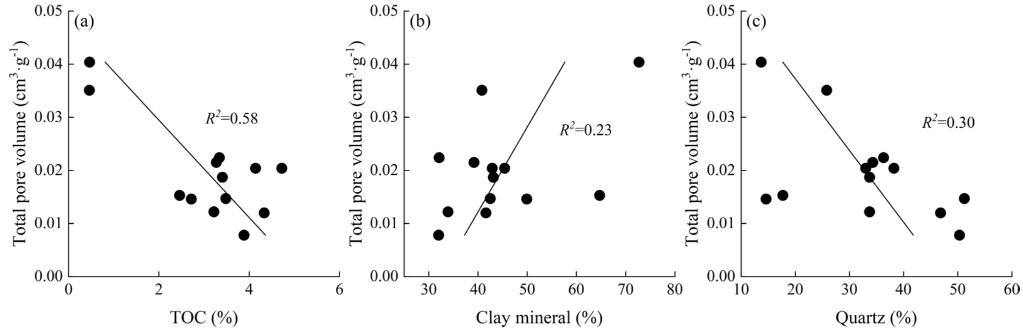

Figure 10. (**a**) Relationship between total pore volume and TOC; (**b**) Relationship between total pore volume and clay mineral; (**c**) Relationship between total pore volume and quartz.

5.3. Fractal Dimension and Pore Structure Relationship

The plots of the fractal dimension and pore structure parameters of shale in the fourth member of Shahejie Formation (Figure 11) show that the specific surface area of shale pores has a significant positive correlation with fractal dimensions D_1 and D_2; R^2 is 0.53 and 0.76, respectively; The average pore diameter has a significant negative correlation with the fractal dimensions D_1 and D_2; R^2 is 0.84 and 0.72, respectively. The total pore volume was positively correlated with fractal dimensions D_1 and D_2; R^2 was 0.30 and 0.64, respectively. This shows that the larger the specific surface area, the smaller the average pore diameter and the larger the total pore volume, the larger the fractal dimension will be, the rougher the inner surface of the pore will become, the more complex the pore structure and the stronger the heterogeneity will be.

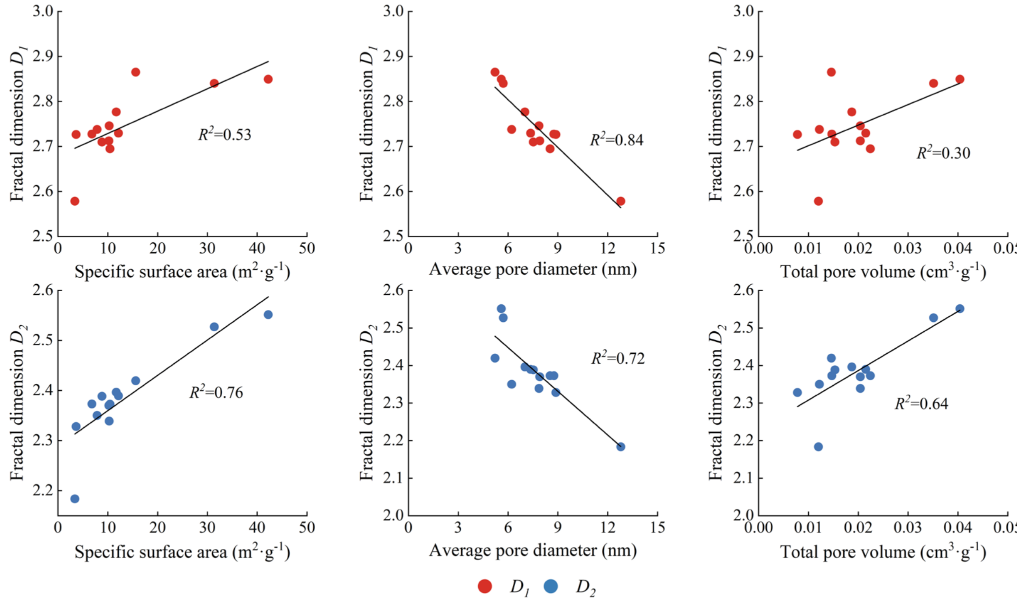

Figure 11. Relationship between pore structure parameters and fractal dimension of Sha-4 shale.

5.4. Factors Influencing Fractal Dimension

The TOC content and mineral composition have a major effect on fractal dimension and micropore structure heterogeneity in shale pores [31]. In the study area, the fractal dimension of the shale pore structure in the fourth member of the Shahejie Formation is mainly affected by TOC and quartz, while the influence of clay minerals on the fractal dimension is relatively weak (Figure 12).

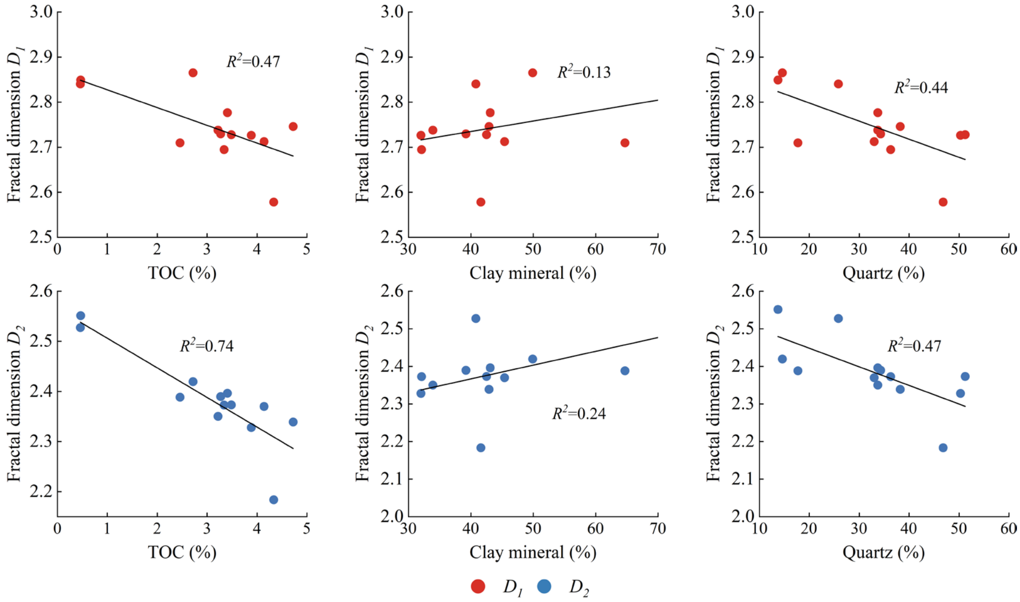

Figure 12. Relationship between fractal dimension and TOC and mineral components.

The fractal dimension and TOC show an obvious negative correlation, that is, the more organic matter content, the smaller the pore fractal dimension and the weaker the heterogeneity of pore structure. The TOC of highly mature marine shale is positively correlated with the fractal dimension, which is mainly associated with the thermal maturity of organic matter; the higher the thermal maturity of organic matter, the more the pores of organic matter are developed [32]. The thermal evolution process of organic matter is a process of consuming organic carbon content [33]. In continental shale rich in organic matter with low maturity, the pores of organic matter are underdeveloped and excessive organic matter is not consumed and filled in the pores [34], leading to the reduction of specific surface area and pore volume inside the pores, thus affecting the pore fractal dimension and heterogeneity.

Clay minerals in continental shale contain a large number of micropores [35,36]. The pores formed by stacking mineral particles are very complex in shape, enhancing the heterogeneity of the shale pore structure. However, there is almost no correlation between clay mineral content and the fractal dimension of shales in the fourth member of the Shahejie Formation in the study area. It is observed by SEM that the shale of the Sha-4 member is often the carrier of organic matter due to its low thermal evolution. Therefore, in terrestrial low maturity organic-rich shales, even if a large number of micropores form between the clay minerals, the low maturity fills a large amount of organic matter, resulting in the influence of the clay minerals on the pore structure, and poor fractal characteristics of the shale being less pronounced.

The fractal dimension of shale pores in the fourth member of the Shahejie Formation shows a negative correlation with the quartz content. Higher quartz content results in a lower fractal dimension. Quartz is not easy to dissolve, which can play a supporting role in pores, reduce the impact of compaction on pores and reduce the degree of heterogeneity of pore structure.

6. Conclusions

(1) The shales in the Liaohe Western Depression are characterized by high TOC, low maturity and high clay mineral content. They are mainly mesoporous. The main pore types are intergranular pores and inter-crystalline pores. The pore morphology is very irregular, mostly flat and slit-shaped. The pore structure of shales has obvious dual fractal characteristics and the pores with larger pore diameters have stronger heterogeneity.

(2) The pore structure and fractal characteristics of continental low mature organic shale are affected by organic matter content. In continental low mature shale, a large amount of organic matter fills in the pores, affecting the pore structure. The higher the content of organic matter, the weaker the heterogeneity of pore structure and the lower the complexity.

(3) Although clay minerals in continental shale can form a large number of micropores, they are filled with organic matter under low maturity conditions and the impact of compaction weakens the impact on pore structure and fractal characteristics of shale. Rigid minerals such as quartz can support and protect pores, provide space for organic matter filling and are not easy to dissolve under low mature conditions, reducing the heterogeneity of pore structure of low mature continental shale.

(4) The influence of the sedimentary environment on the micropore structure of shale is specifically reflected in the difference in mineral components and the level of maturity, especially the influence of maturity, which controls the type of pore development in shale and also directly affects the role of organic matter in the genetic mechanism of shale microheterogeneity.

Author Contributions: Conceptualization, Y.L. and L.Z.; methodology, L.Z. and X.Z.; validation, Y.L. and L.Z.; formal analysis, Y.L. and Y.X.; investigation, F.J. and Y.W.; resources, L.Z. and J.L.; data curation, L.Z. and X.H.; writing—original draft preparation, Y.L.; writing—review and editing, Y.L. and L.Z.; visualization, Y.L.; supervision, Y.L. and L.Z.; funding acquisition, L.Z. All authors have read and agreed to the published version of the manuscript.

Funding: This research was funded by Natural Science Foundation of Chongqing, China, grant number cstc2020jcyj-msxmX0657 and National Natural Science Foundation of China, grant number 41672113.

Data Availability Statement: Not applicable.

Conflicts of Interest: The funders had no role in the design of the study; in the collection, analyses, or interpretation of data; in the writing of the manuscript; or in the decision to publish the results.

References

1. Shao, X.H.; Pang, X.Q.; Hu, T.; Xu, T.W.; Xu, Y.; Tang, L.; Li, H.; Li, L.L. Microscopic characteristics of pores in Es-3 shales and its significances for hydrocarbon retention in Dongpu Sag, Bohai Bay Basin. *Oil Gas Geol.* **2019**, *40*, 67–77.
2. Jarvie, D.M.; Hill, R.J.; Ruble, T.E.; Tim, E.R. Unconventional shale-gas systems:The Mississippian Barnett Shale of north-central Texas as one model for thermogenic shale-gas assessment. *AAPG Bull.* **2007**, *91*, 475–499. [CrossRef]
3. Roger, M.S.; Neal, R.O. Pore types in the Barnett and Woodford gas shales:Contribution to understanding gas storage and migration pathways in fine-grained rocks. *AAPG Bull.* **2011**, *95*, 2017–2030.
4. Chen, S.B. Study review on microstructure and adsorption heterogeneity of shale reservoir. *Coal Sci. Technol.* **2016**, *44*, 23–32. [CrossRef]
5. Wang, H.; Shi, Y.M.; Xu, D.W.; Chen, X.; Li, L.M.C.D. Characterization techniques and progress of unconventional reservoir pore structure. *Pet. Geol. Recovery Effic.* **2019**, *26*, 21–30. [CrossRef]
6. Cheristine, E.K. Fractal measurements of sandstones, shales, and carbonates. *J. Geophys. Res. Solid Earth* **1988**, *93*, 3297–3305.
7. Xiong, J.; Liu, X.J.; Ling, L.X. Pore Structure and Fractal Characteristics of Longmaxi Formation Shale in the Changning Region of Sichuan Basin. *Geol. Sci. Technol. Inf.* **2015**, *34*, 70–77.
8. Ji, W.M.; Song, Y.; Jiang, Z.X.; Meng, M.M.; Liu, Q.X.; Chen, L.; Wang, P.F.; Gao, F.L.; Huang, H.X. Fractal characteristics of nano-pores in the Lower Silurian Longmaxi shales from the Upper Yangtze Platform, south China. *Mar. Pet. Geol.* **2016**, *78*, 88–98. [CrossRef]
9. Nie, W.C.; Zhang, T.S.; Wang, M.W.; Wu, W.; Tan, X.C. Fractal Characteristics and Interfering Factors of Microscopic pores in Marine-continental Transitional Coal Shale: A case study of the Taiyuan Formation in the northern Qinshui Basin. *Acta Sedimentol. Sin.* **2022**, *78*, 1000–0550.
10. Yin, L.L.; Guo, S.B. Full-Sized Pore Structure and Fractal Characteristics of Marine-Continental Transitional Shale: A Case Study in Qinshui Basin, North China. *Acta Geol. Sin.-Engl. Ed.* **2019**, *93*, 675–691. [CrossRef]
11. Sun, Y.S.; Guo, S.B. Qualitative and Quantitative Characterization of Shale Microscopic Pore Characteristics Based on Image Analysis Technology. *Adv. Earth Sci.* **2016**, *31*, 751–763.
12. Li, X.G.; Chen, Y.C.; Li, Y.J.; Lan, K.; Li, J.H.; Gong, W.M. Petroleum Exploration History and Enlightenment of Liaohe Depression in Bohai Bay Basin. *Xinjiang Pet. Geol.* **2021**, *42*, 291–301.
13. Liu, S.Q.; Jiang, Z.X.; Wang, X.B.; Chen, J.; Gao, Y.; Wu, M.H.; Sun, X.W.; Luan, T.S. Reservoir Characteristics and the Effect of Diagenesis on E2s4 Reservoir in the West Slope of West Depression, Liaohe Oilfield. *Geoscience* **2015**, *29*, 692–701.
14. Ge, M.N.; Zhang, J.C.; Li, W.J.; Sun, R. Main controlling factors analysis of shale oil and gas accumulation in west sag of Liaohe depression. *Pet. Geol. Eng.* **2015**, *29*, 46–49+53+146.
15. Yang, C.; Zhang, J.C.; Li, W.J.; Jing, T.Y.; Sun, R. Microscopic pore characteristics of Sha-3 and Sha-4 shale and their accumulation significance in Liaohe Depression. *Oil Gas Geol.* **2014**, *35*, 286–294.
16. Shan, Y.S.; Zhang, J.C.; Li, X.G.; Bi, C.Q.; Tang, Y. Hydrocarbon enrichment conditions and distribution in continental shale, West Liaohe Sag, Bohai Bay Basin. *Pet. Geol. Exp.* **2016**, *38*, 496–501.
17. Chen, C.; Jin, K.; Lei, W.W.; Wang, H.; Guo, F.; Qian, L.X.; Qin, X.C. High-precision Prediction of Thin Sandstones in Dujiatai Oil Layer of Shuguang Area. *Spec. Oil Gas Reserv.* **2020**, *27*, 96–101.
18. Song, B.; Wang, B.; Liu, X.Z.; Liu, S.Z.; Chen, X.G.; Lu, W.Z. Genetic Types and Distribution Rules of Thin Sand Layers in the Fourth Member of Shahejie Formation in Shubei Area of the Western Sag, Liaohe Depression. *Geol. Resour.* **2021**, *30*, 698–706.
19. Xue, S.H.; Luo, P.; Yang, Y.T.; Xu, T.G. Depositional systems and oil/gas distribution in the Liaohe Depression. *Pet. Explor. Dev.* **1997**, *24*, 19–22.
20. Mao, J.L.; Jing, T.Y.; Han, X.; Shang, C.; Huang, S.Q.; Ma, M.X. Petrology types and organic geochemical characteristics of shale in the Western Depression, Liaohe. *Earth Sci. Front.* **2016**, *23*, 185–194.
21. Ge, X.B.; Li, J.J.; Lu, S.F.; Chen, F.W.; Yang, D.X.; Wang, Q. Fractal characteristics of tight sandstone reservoir using mercury intrusion capillary pressure:a case of tight sandstone reservoir in Jizhong Depression. *Lithol. Reserv.* **2017**, *29*, 106–112.
22. Liu, J.P.; Liu, D.X.; Hu, H.Y.; Qiao, P.F.; Wang, T.; Xie, Z.T.; Liu, L.H. Pore structure characteristics of marine continental transitional facies shale of Shanxi formation in the eastern margin of Ordos basin. *China Sci.* **2022**, *17*, 21–30.
23. Liu, X.P.; Jin, Z.J.; Lai, J.; Fan, X.C.; Guan, M.; Shu, H.L.; Wang, G.C. Fractal behaviors of NMR saturated and centrifugal T2 spectra in oil shale reservoirs: The Paleogene Funing formation in Subei basin, China. *Mar. Pet. Geol.* **2021**, *129*, 105069. [CrossRef]
24. Liu, K.Q.; Ostadhassan, M.; Kong, L.Y. Fractal and Multifractal Characteristics of Pore Throats in the Bakken Shale. *Transp. Porous Media* **2019**, *126*, 579–598. [CrossRef]
25. Liu, K.Q.; Ostandhassan, M.; Jang, H.W.; Zakharova, N.V.; Shokouhimehr, M. Comparison of fractal dimensions from nitrogen adsorption data in shale via different models. *RSC Adv.* **2021**, *11*, 2298–2306. [CrossRef]
26. Li, Z.Q.; Wang, W.; Wang, X.M.; Bai, Y.W.; Qin, D.T.; Zhao, Y. Study on fractal characteristics of micro-nano pore structure of shale. *J. Eng. Geol.* **2018**, *26*, 494–503.
27. Zhu, H.Q.; Jia, A.L.; Wei, Y.S.; Jia, C.Y.; Yuan, H. Microscopic Pore Structure and Fractal Characteristics of Wufeng-Longmaxi Shale, South Sichuan. *Sci. Technol. Eng.* **2018**, *18*, 12–19.

28. Matthias, T.; Katsumi, K.; Alexander, V.N.; James, P.O.; Francisco, R.-R.; Jean, R.; Kenneth, S.W.S. Physisorption of gases, with special reference to the evaluation of surface area and pore size distribution(IUPAC Technical Report). *Pure Appl. Chem.* **2015**, *87*, 1051–1069.
29. Wang, M.; Xue, H.T.; Tian, S.S.; Ronald, W.T.W.; Wang, Z.W. Fractal characteristics of Upper Cretaceous lacustrine shale from the Songliao Basin, NE China. *Mar. Pet. Geol.* **2015**, *67*, 144–153. [CrossRef]
30. Yang, F.; Ning, Z.F.; Wang, Q.; Kong, D.T.; Peng, K.; Xiao, L.F. Fractal Characteristics of Nanopore in Shales. *Nat. Gas Geosci.* **2014**, *25*, 618–623.
31. Chang, J.Q.; Fan, X.D.; Jiang, Z.X.; Wang, X.M.; Chen, L.; Li, J.T.; Zhu, L.; Wan, C.X.; Chen, Z.X. Differential impact of clay minerals and organic matter on pore structure and its fractal characteristics of marine and continental shales in China. *Appl. Clay Sci.* **2022**, *216*, 106334. [CrossRef]
32. Guo, Y.; Zhao, D.F. Study on micro-heterogeneity of marine shale reservoir in micro scale. *J. China Univ. Min. Technol.* **2015**, *44*, 300–307.
33. Ma, M.; Chen, G.J.; Xu, Y.; Hu, S.J.; Lv, C.F.; Xue, L.H. Fractal characteristics of pore structure of continental shale in the process of thermal evolution. *Coal Geol. Explor.* **2017**, *45*, 41–47.
34. Hou, H.h.; Shao, L.y.; Li, Y.H.; Li, Z.; Zhang, W.L.; Wen, H.J. The pore structure and fractal characteristics of shales with low thermal maturity from the Yuqia Coalfield, northern Qaidam Basin, northwestern China. *Front. Earth Sci.* **2018**, *12*, 148–159. [CrossRef]
35. Fu, J.j.; Guo, S.B.; Gao, Q.F.; Yang, J. Reservoir characteristics and enrichment conditions of shale gas in the Carboniferous-Permian coal-bearing formations of Qinshui Basin. *Earth Sci. Front.* **2016**, *23*, 167–175.
36. Song, Y.; Gao, F.l.; Tang, X.L.; Chen, L.; Wang, X.M. Influencing factors of pore structure differences between marine and terrestrial shale reservoirs. *Acta Pet. Sin.* **2020**, *41*, 1501–1512.